Journal of Applied Polymer Science

Morphology and dynamical mechanical properties of poly ether ketone ketone (PEKK) with meta phenyl links

Luis Quiroga Cortés, Nicolas Caussé, Eric Dantras, Antoine Lonjon, Colette Lacabanne
Physique Des Polymères, Institut Carnot CIRIMAT, Université De Toulouse, Toulouse Cedex 09, 31062, France
Correspondence to: A. Lonjon (E-mail: antoine.lonjon@univ-tlse3.fr)

ABSTRACT: Poly ether ketone ketone (PEKK) with different proportion of meta phenyl links were investigated by combining differential scanning calorimetry and dynamic mechanical analysis. The influence of the Terephthalyl/Isophthalyl isomers (T/I) ratio on the vitreous phase is mild, the shift of the glass transition is limited to a few degrees and the vitreous G′ is only sensitive to the content of the crystalline phase. Contrarily, the increase of meta isomers is responsible for a significant decrease of the melting temperature (T_m) by 60 °C, which considerably facilitates processing. The modification of interchain interactions in the crystalline phase might be implied. A series of thermal protocols evidenced that the difference of crystallization behavior is also dependent upon the T/I isomer ratio. A time and temperature dependence of annealing on the double melting behavior of PEKK was observed. Regarding the mechanical behavior, the observed reinforcing effect due to the crystalline phase was more prominent in the rubbery state than in the glassy state. © 2016 Wiley Periodicals, Inc. J. Appl. Polym. Sci. **2016**, *133*, 43396.

KEYWORDS: composites; crystallization; properties and characterization; thermoplastics

Received 24 September 2015; accepted 30 December 2015
DOI: 10.1002/app.43396

INTRODUCTION

There is an increasing interest in thermoplastic polymers as composite matrices in the aeronautics and space industries. Thermoplastic composites not only allow important weight savings but they also exhibit high mechanical strength and good environmental resistance. In this context, properties of poly aryl ether ketones (PAEKs) polymers draw the attention for high performance composites.[1,2] The PAEK family bring together polymers with a linear chain composed of alternating aromatic rings and ketone or ether groups. Their structure provides them good thermal, chemical, and mechanical properties.[3,4] The most extensively studied is poly ether ether ketone (PEEK).[5] PEEK has a glass transition temperature (T_g) of 144 °C and a melting temperature (T_m) of 340 °C.[2] Throughout last decades, PEEK was one of the main candidates as matrix for advanced composites.[6–8] Another member of this polymer family, poly ether ketone ketone (PEKK),[2,9,10] has received great interest as an alternative to PEEK.[9,11–13] PEKK was originally developed by Dupont;[14] it exhibits a high glass transition temperature, T_g, of 156 °C and a melting point, T_m, of 360 °C to 380 °C.[2] It can be obtained in amorphous or semicrystalline form, with different para/meta phenyl isomer ratios, by Friedel-Crafts polymerization[4] from diphenyl ether, terephthaloyl, and isophthaloyl chloride. The higher content of ketone linkages in PEKK can explain higher values of T_g and T_m; ketone linkages are more rigid than ether.[15,16] One of the principal advantages of PEKK over PEEK is that the melting point can be modulated, as revealed by Gardner.[17] The 100% para PEKK and para - meta PEKK show differences in crystallinity behavior and melting point temperature, while the glass transition temperature stays quasi-constant. With increasing meta isomers, the defects or the disruption caused by meta isomers in the crystalline packing decrease the melting temperature as well as the crystallization rate. For industrial applications, this is an important point because lowering processing temperatures not only facilitates composites manufacturing[18] but also prevent the material degradation.

Great attention was given to the influence of processing conditions on crystallization behavior.[17,19–21] PEKK is a semi crystalline polymer and its crystallinity strongly depends on the thermal history and processing conditions. For example, by quenching from the melt, PEKK can be obtained in the quasi-amorphous state whereas a semi crystalline PEKK can be obtained with slow cooling conditions or by isothermal crystallization between T_g and T_m. In the case of specific thermal protocols, a double melting behavior has been observed in PEKK[17] as in other semicrystalline polymers like PEEK[22] or Poly Ethylene Terephtalate.[23] The dynamic mechanical analyses of PAEK were performed[24–26] in previous works. However, to the best of our knowledge, study of PEKK crystallization behavior by combined thermal and

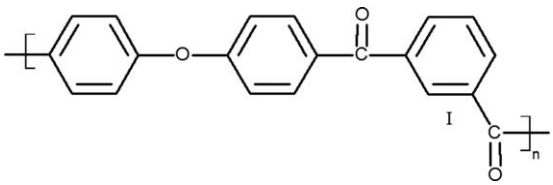

Figure 1. Molecular structure of PEKK with meta links.

mechanical analysis has never been done. Here, we propose an extensive study with three different grades of PEKK in order to study the influence of different thermal protocols on crystallization. Then dynamic mechanical properties will be examined as a function of the physical structure.

EXPERIMENTAL

Materials

PEKK (Figure 1) was supplied by ARKEMA France in powder form (20 μm). Three references, PEKK KEPSTAN 8002, PEKK KEPSTAN 7003, and PEKK KEPSTAN 6003, were studied. The three grades have similar chemical structure but they differ by their Terephthalyl/Isophthalyl isomers ratio, noted T/I ratio. For PEKK KEPSTAN 8002, 7003, and 6003, the T/I ratios are 80/20, 70/30, and 60/40, respectively. Samples were performed directly from the powder in a hot press. PEKK 80/20, 70/30, and 60/40 were melted at 390 °C, 370 °C, and 340 °C respectively during 10 min and then pressed at 1 MPa to obtain 500 μm thickness films.

Methods

Differential Scanning Calorimetry. Differential scanning calorimetry measurements were performed using a calorimeter 2920 from Thermal Analysis instruments. The samples weight varied from 5 to 15 mg. They were analyzed in non-hermetically sealed aluminum pans. Scans were achieved under dry nitrogen. The first heating consisted to erase the thermal history of the polymer at 380 °C. Only the second heating was considered for data analysis. The cooling and the heating rate were 10 °C min^{-1} unless otherwise specified in the temperature range of 50 °C to 400 °C. For isothermal crystallization study, PEKK samples were annealed at 230 °C, 245 °C, and 255 °C from 10 to 60 min. The crystallinity χ_c of PEKK polymer can be estimated with:

$$\chi_c = \frac{\Delta H_m - \Delta H_{cc}}{\Delta H_{100\%}} \times 100, \quad (1)$$

where ΔH_m melting enthalpy, ΔH_{cc} cold crystallization enthalpy, and $\Delta H_{100\%}$ melting enthalpy of the theoretical 100% crystalline polymer. According with Chang *et al.* the enthalpy of melting of PEKK ($\Delta H_{100\%}$) considered as 100% crystalline is approximately 130 J g^{-1}.[9]

Dynamic Mechanical Analysis. The dynamic mechanical properties of PEKK samples were determined using an ARES strain controlled rheometer from Thermal Analysis Instruments in the rectangular torsion mode. Shear dynamic mechanical storage modulus and loss modulus, G′ and G″, were recorded as a function of temperature. Measurements were achieved in a temperature range of −130 to 270 °C, with a scanning rate of 3 °C min^{-1}. The angular frequency (ω) was 1 rad s^{-1} and the strain (γ) was 10^{-1}%. Semicrystalline samples were obtained by annealing amorphous films at 245 °C in an oven for different times.

Test samples had parallelepiped shape with a length of ca 30 mm, a width of ca 10 mm, and a thickness of ca 500 μm.

RESULTS

Transitions

Differential scanning calorimetry analysis of PEKK 60/40, 70/30, and 80/20 were performed with a cooling and heating rate of 10 °C min^{-1}. Only the heating scans are reported (Figure 2). PEKK 80/20 has a T_g of 161 ± 1 °C and a melting endotherm at 360 ± 1 °C (ΔH_m = 43 ± 1 J g^{-1}). PEKK 70/30 has a T_g of 159 ± 1 °C and shows a melting endotherm at 335 ± 1 °C (ΔH_m = 35 ± 2 J g^{-1}). PEKK 60/40 has a T_g of 156 ± 1 °C and also present a melting endotherm at 300 ± 1 °C (ΔH_m=17 ± 3 J g^{-1}). PEKK 60/40 exhibits a cold crystallization above the glass transition at T_{cc} = 241 ± 2 °C (ΔH_{cc}=13 ± 3 J g^{-1}). The crystallinity ratio is 3 ± 2% for 60/40, 27 ± 2% for 70/30, and 33 ± 1% for 80/20, where 60/40 is a quasi-amorphous polymer, 70/30 and 80/20 are semicrystalline polymers. An enthalpy overshoot is superimposed on the heat capacity step for PEKK 60/40 but not for the 70/30 or 80/20. This behavior is associated with the physical ageing phenomenon.[27,28]

In order to study the influence of thermal history on PEKK physical structure, the different grades of PEKK were submitted to various cooling rates in the Differential Scannig Calorimetry set up. After these cooling steps, DSC thermograms on heating at 10 °C min^{-1} were monitored and reported for PEKK 60/40 [Figure 3(a)], PEKK 70/30 [Figure 3(b)], and PEKK 80/20 [Figure 3(c)]. Quenched samples were directly cooled in liquid nitrogen from the melt. All data are listed in Table I. PEKK 60/40 samples cooled at a low rate (lower than 2 °C min^{-1}) do not show any cold crystallization process. They possess also high levels of crystallinity. From a cooling rate of 5 °C min^{-1}, cold crystallization process occurs. Upon increasing of the cooling rate, the crystallization enthalpy increases, the cold crystallization temperature shifts to higher temperatures. For PEKK

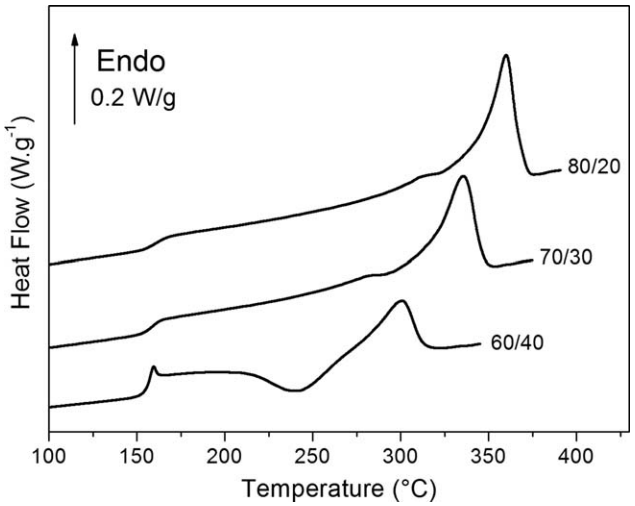

Figure 2. DSC thermograms at 10 °C min^{-1} for PEKK 60/40, 70/30, and 80/20.

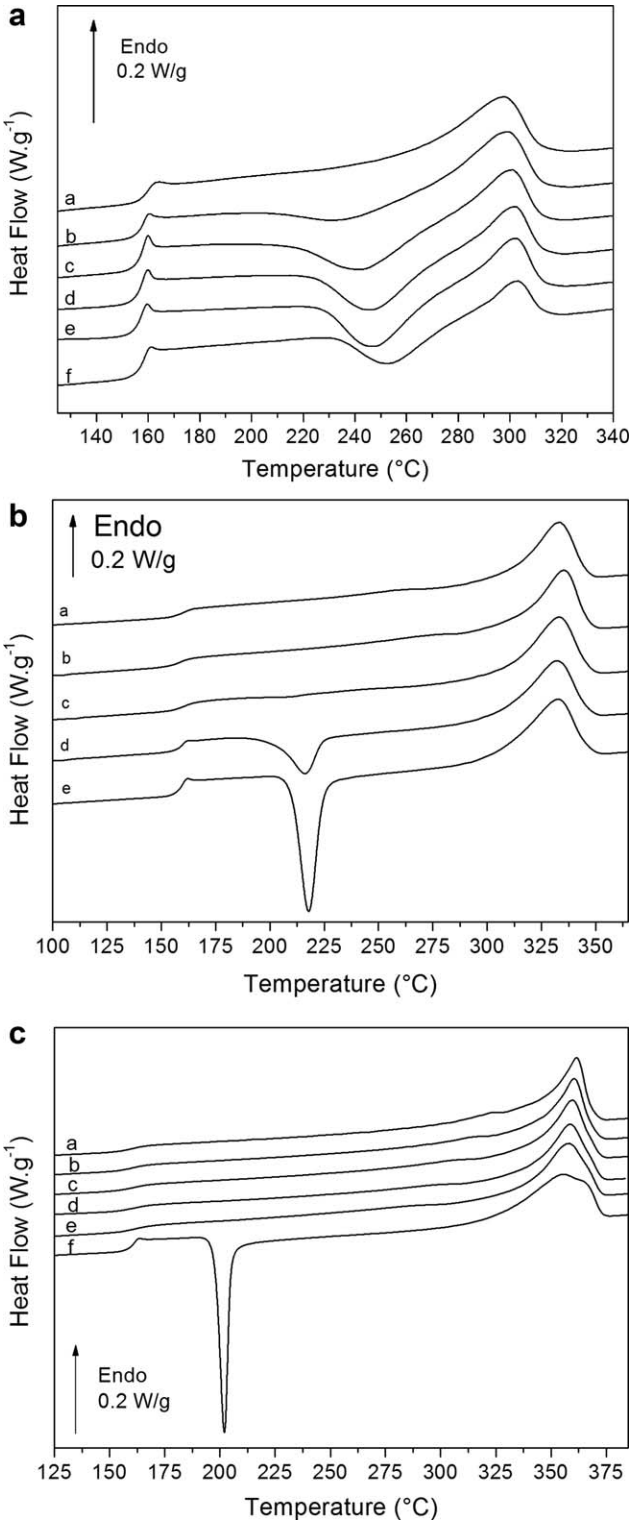

Figure 3. (A) DSC thermograms of PEKK 60/40 at 10 °C min^{-1} after different cooling rates: (a) 2 °C min^{-1}, (b) 5 °C min^{-1}, (c) 10 °C min^{-1}, (d) 20 °C min^{-1}, (e) 40 °C min^{-1}, and (f) quenched. (B) DSC thermograms of PEKK 70/30 at 10 °C min^{-1} after different cooling rates: (a) 10 °C min^{-1}, (b) 20 °C min^{-1}, (c) 40 °C min^{-1}, (d) 60 °C min^{-1}, and (e) quenched. (C) DSC thermograms of PEKK 80/20 at 10 °C min^{-1} after different cooling rates: (a) 5 °C min^{-1}, (b) 10 °C min^{-1}, (c) 20 °C min^{-1}, (d) 40 °C min^{-1}, (e) 60 °C min^{-1}, and (f) quenched.

70/30, only rapidly cooled samples exhibit cold crystallization endotherm. This phenomenon is not detected for cooling rates lower than 40 °C min^{-1}. For PEKK 80/20, only the quenched sample exhibits the cold crystallization endotherm. When the cold crystallization process appears, it starts earlier in temperature for amorphous PEKK 80/20 (190 °C) than for amorphous 70/30 (200 °C) or amorphous 60/40 (230 °C). For all PEKK grades, no significant evolution is noted for the melting point with increasing cooling rate. The crystallinity ratio decreases with increasing cooling rate (Table I). For PEKK 60/40, the crystallinity varies from 14% for a slow cooling rate of 5 °C min^{-1} to 0.5% after quenching into liquid nitrogen. It decreases from 28% to 3% and from 34% to 7% for PEKK 70/30 and 80/20, respectively. Comparing with same cooling rates, PEKK 80/20 is able to develop more crystalline phase. The glass transition temperatures, T_g, are also reported on Table I, there is no significant evolution as a function of cooling rates. The rapidly cooled samples thermograms show an endothermic peak superimposed on the glass transition step. In PEKK 60/40, the peak intensity increases when the cooling rate slows down (between the quenched sample and the one cooled at 10 °C min^{-1}) as can be expected from an overshoot characteristic of physical ageing. This phenomenon will not be discussed deeply because the samples do not exhibit constant crystallinity ratio.

DSC thermograms of quasi-amorphous PEKK 60/40 annealed for various times and temperatures above T_g are reported (Figures 4 and 5). The crystallinity before annealing was estimated at 2%. Quasi-amorphous samples were heated at 210, 220, 230, 240, 250, and 260 °C for 60 min (Figure 4), or heated at 245 °C for 5, 10, 20, 40, and 60 min (Figure 5). Then, samples were scanned between 100 °C and 350 °C. Data extracted from these thermograms are listed in Table II. No specific variation of T_g is observed with increasing annealing time or temperature. After the annealing step, two endotherms are observed above T_g: the classic melting, called the higher temperature endotherm (HTE), and a small peak, called the lower temperature endotherm (LTE). With increasing annealing time or temperature, the LTE peak maximum shifts to higher temperatures. The LTE appears at 221 ± 1 °C for an annealing at 210 °C and increases up to 269 ± 1 °C for an annealing at 260 °C. For a 5 min annealing at 245 °C, the LTE appears at 251.5 ± 1 °C and increases up to 256 ± 1 °C after a 60 min annealing. For various annealing temperatures, the LTE maximum appears 10 °C above the annealing temperature. The temperature of the HTE remains constant in all experiments. The crystallinity of samples is determined thanks to eq. (1) after the annealing treatment. The total area under the two endotherms is used to determine the melting enthalpy. A quasi-amorphous sample reaches a crystallinity ratio about 22% after a 5 min annealing at 245 °C. The enthalpy corresponding to the low melting endotherm increases with increasing annealing time and temperature. Samples reach a crystallinity ratio of 27% for long annealing duration or high temperature annealing.

Mechanical Relaxations

Dynamic mechanical analyses of PEKK 60/40, 70/30, and 80/20 were performed on samples cooled from the melt into two aluminum plates at room temperature during manufacturing

Table I. Transitions Temperatures, Enthalpies, and Crystallinity Ratio of for PEKK Samples Submitted at Various Cooling Rates

Cooling rate (°C min^{-1})	T_g (°C)	T_{cc} (°C)	ΔH_{cc} (J g^{-1})	T_m (°C)	ΔH_m (J g^{-1})	χ (%)
PEKK 60/40						
0.5	158.5	x	x	296.5	36.9	28.4
1	157.5	x	x	297.5	35.2	27.0
2	158.0	x	x	298.0	28.1	21.6
5	156.5	231.0	3.8	299.5	22.1	14.1
10	156.5	240.5	13.4	300.0	16.7	2.5
20	156.0	244.5	12.5	301.5	16.1	2.7
40	156.5	247.0	12.2	301.5	15.4	2.5
60	155.5	244.5	13.8	301.0	17.0	2.5
Quenched	157.5	253.5	8.8	302.5	9.5	0.5
PEKK 70/30						
10	159.0	x	x	336.0	36.0	27.7
20	158.5	x	x	333.5	36.5	28.1
40	160	215.0	1.0	335.5	33.8	25.2
60	159	216.0	13.2	332.0	33.8	15.8
Quenched	158.5	218.0	30.1	332.5	34.4	3.2
PEKK 80/20						
5	160.5	x	0.0	361.5	44.2	34.0
10	160.0	x	0.0	360.5	44.0	33.8
20	161.0	x	0.0	359.5	43.2	33.2
40	160.5	x	0.0	358.5	42.7	32.9
60	161.0	x	0.0	358.5	41.0	31.5
Quenched	160.0	202.0	31.6	355.5	40.8	7.1

process. The crystallinity previously determined by DSC is 1.5 ± 1% for PEKK 60/40, 8 ± 1% for 70/30, and 29% ± 1 for 80/20. Dynamic Mechanical Analysis thermograms are reported as a function of temperature on Figure 6, where Figure 6(a) corresponds to G′, and Figure 6(b) to G″. In Figure 6(a), on the vitreous plateau, G′ follows an approximately linear course around 1 GPa for the different meta phenyl links content. At −125 °C, the value of G′ is 1.5 ± 0.2 GPa for 60/40, 1.4 ± 0.2 GPa for 70/30, and 2 ± 0.2 GPa for 80/20. At +125 °C, G′ values are 1.0 ± 0.1 GPa for 60/40, 0.9 ± 0.1 GPa for 70/30, and 1.3 ± 0.2 GPa. No significant difference is observed for the PEKK grades between −130 °C and 140 °C. After 140 °C, the observed sudden drop corresponds to the viscoelastic transition associated with the mechanical manifestation of the glass

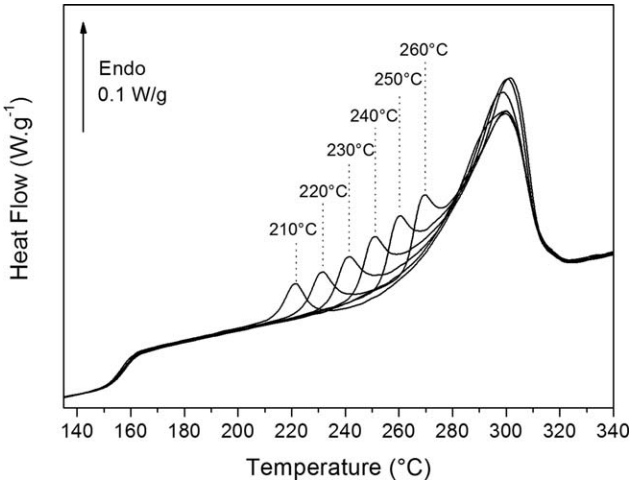

Figure 4. DSC thermograms of isothermally crystallized PEKK 60/40 at 210, 220, 230, 240, 250, and 260 °C for 60 min.

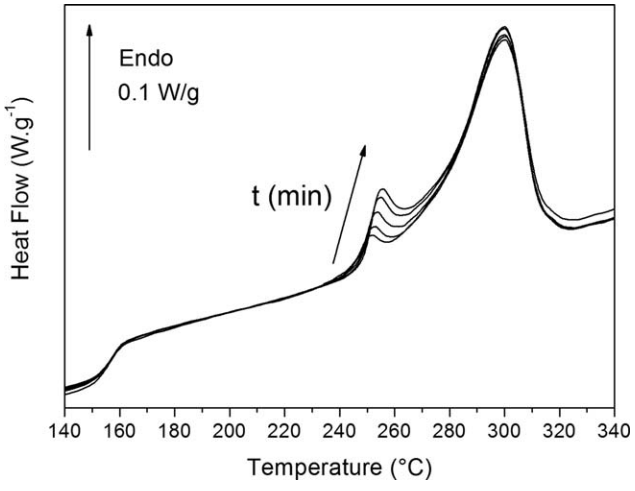

Figure 5. DSC thermograms of isothermally crystallized PEKK 60/40 at 245 °C for 5, 10, 20, 40, and 60 min.

Table II. Transitions Temperatures, Enthalpies, and Crystallinity Ratio of PEKK 60/40 after Annealing Process

Sample – PEKK 6003	T_g (°C)	LTE (°C)	HTE (°C)	ΔH_m (J g^{-1})	χ (%)
210 °C – 60 min	158.0	221.0	300.0	28.9	22.2
220 °C – 60 min	157.5	231.5	300.0	31.6	24.3
230 °C – 60 min	157.0	241.5	299.5	34.0	26.2
250 °C – 60 min	156.5	260.0	300.5	35.5	27.3
260 °C – 60 min	156.5	270.0	301.5	34.5	26.5
245 °C – 5 min	155.5	251.5	300.0	29.3	22.5
245 °C – 10 min	156.0	252.5	300.0	30.4	23.4
245 °C – 20 min	156.5	253.5	300.0	31.8	24.5
245 °C – 40 min	156.5	255.0	300.0	33.3	25.6
245 °C – 60 min	156.5	255.5	300.5	34.3	26.4

transition: it is designated as α-relaxation. For 60/40 and 70/30 T/I ratio, the drop of G′ is about 2.5 decades, between 140 °C and 170 °C. For PEKK 80/20, the drop of G′ is of one decade between 140 °C and 190 °C. The above differences on viscoelastic steps as a function of T/I ratio, are consistent with the evolution of crystallinity.

Between 170 °C and 190 °C, the rubbery plateau of PEKK 60/40 and 70/30 is observed. The decrease of G′ with increasing temperature on this plateau can be related to a beginning of flow-like behavior at a microscopic scale. This phenomenon is blocked by a sufficient percentage of crystallinity e.g. for PEKK 80/20. In the case of PEKK 60/40, the cold crystallization process occurs at 210 °C and the G′ increases for about 2.5 decades. The same phenomenon is noticed for PEKK 70/30 at 190 °C and the increase of G′ is about 1.5 decades.

At higher temperature, the rubbery plateau of semi-crystalline PEKK 70/30 and 80/20 is observed at 50 and 90 ± 5 MPa. For PEKK 60/40, there is no true rubbery plateau: a maximum value of G′ is reached—50 MPa—and then G′ decreased due to the beginning of the melt process.

The evolution of G″ versus temperature [Figure 6(b)] is equivalent between −130 °C and 140 °C for the different grades of PEKK. At low temperature, the two G″ maxima correspond to secondary relaxations noted γ and β, respectively, located at $T_\gamma = -96 \pm 1$ °C and $T_\beta = -33 \pm 1$ °C, respectively. The temperatures and the intensities of these secondary relaxations are almost the same for the different PEKK grades. In the high temperatures region, the α mode is observed. T_α value is 154 ± 1 °C for PEKK 60/40, 157 ± 1 °C for 70/30, and 161 ± 1 °C for 80/20. Those values are consistent with T_g values measured by DSC (Figure 2). For PEKK 60/40 and 70/30, G″ drops by two orders of magnitude after T_α to such a low value that the sensitivity limit of the apparatus is reached. At 190 °C for 70/30 and 215 °C for 60/40, G″ increases due to the influence of cold crystallization. Instead of PEKK 60/40 and 70/30, G′ drops one decade after T_α for PEKK 80/20.

The shear modulus of PEKK 60/40 has been compared during the first and the second temperature scans (Figure 7). Samples were equilibrated for a couple of hours at room temperature between the two scans to reach the same equilibrium state before the analysis. The only varying parameter is the crystallinity of PEKK samples, determined by DSC before the scan. For the first scan, the crystallinity value is close to 1.5 ± 1%. Before second scan, the achieved crystallinity is 23% ± 1% due to cold crystallization during the first scan. The modulus on the vitreous plateau is slightly higher for the crystalline sample where, at −125 °C the

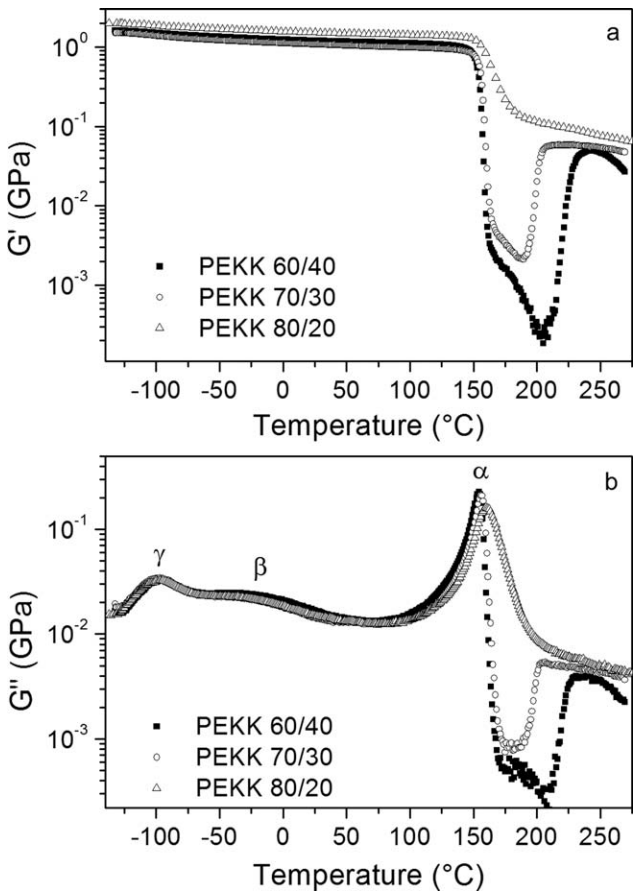

Figure 6. (a) G′ versus temperature at 1 rad s^{-1} for PEKK 60/40, 70/30, and 80/20. (b) G″ versus temperature at 1 rad s^{-1} for PEKK 60/40, 70/30, and 80/20.

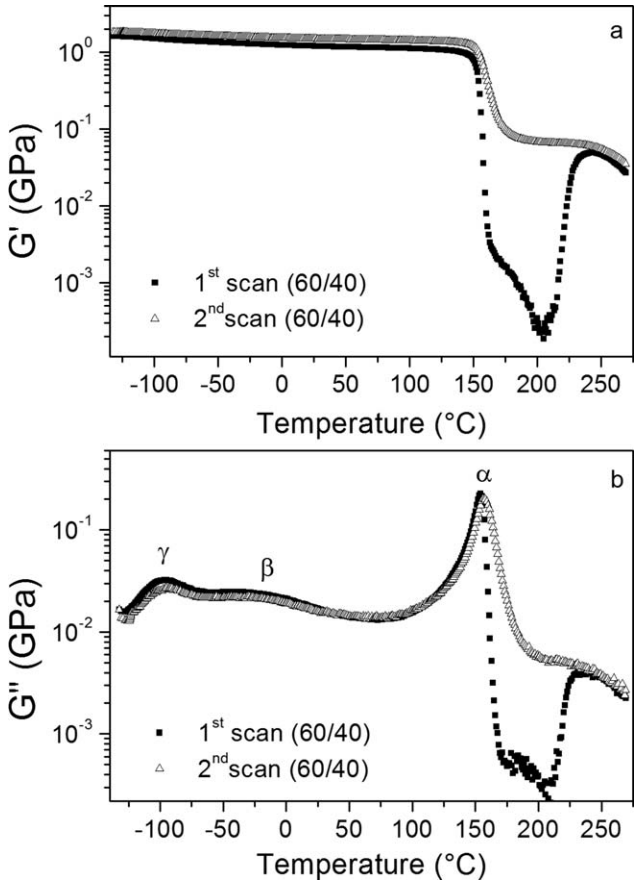

Figure 7. (a) G′ versus temperature at 1 rad s^{-1} for PEKK 60/40 at first and second scan. (b) G″ versus temperature at 1 rad s^{-1} for PEKK 6003 at first and second thermogram.

value is 1.8 GPa ± 0.2 and 1.5 GPa ± 0.2 at +125 °C. As seen previously, G′ of the quasi-amorphous sample shows a severe decrease associated with the viscoelastic transition between 140 °C and 170 °C from 1 GPa to 3 MPa. At second scan, this drop is noticed from 1.5 GPa to 70 MPa. At the end of the rubbery plateau at 250 °C, G′ decreases due to the beginning of the melting process. In Figure 7(b), the evolution of G″ for both scans are reported. The γ and the β modes show no differences in peak temperature and magnitude between the crystalline and the quasi-amorphous sample. It is observed that the value of T_α is slightly higher for the crystalline sample (156 °C) than for the amorphous one (154 °C). Finally, the α mode is broadened asymmetrically towards higher temperatures between the first and second scan.

The thermal annealing time influence on the mechanical properties has been explored on PEKK 60/40. The evolution of the real part G′ and the imaginary part G″ of the shear modulus is reported versus temperature in Figure 8(a,b), respectively. Quasi-amorphous samples of PEKK 6003 were previously isothermally crystallized at 245 °C for different times to reach the following crystallinity ratios: 10.5%, 20%, 25%, and 27.5% for 5, 10, 30, and 60 min, respectively (see Table III). Below T_∞ G′ increases with increasing annealing times. For the amorphous sample, G′ equals 1.5 ± 0.2 GPa at −125 °C and 1 ± 0.1 GPa at +125 °C. For annealed samples, G′ rises up to 2.2 ± 0.2 GPa at −125 °C and 1.6 ± 0.2 GPa at +125 °C. After T_∞ amorphous and crystallized samples curves exhibit different behaviors. By increasing annealing time, the drop of G′ at T_α between 140 °C and 180 °C is highly reduced. The level of the rubbery plateau increases with annealing time from 1 MPa, for the quasi-amorphous sample, to 100 MPa for the 60 min annealed sample. An increase of G′ with temperature associated with cold crystallization is observed after T_α at 180 °C for the amorphous and the 5 min annealed samples. This increase is not observed for the most crystalline samples. Figure 8(b) shows the evolution of G″ versus temperature in the α relaxation region (no influence of the annealing times is observed on the sub-α relaxations). With increasing annealing time, the α peak broadens asymmetrically towards high temperatures. T_α values and α peak intensity are not dependent upon the annealing time.

DISCUSSION

Physical Structure: Amorphous Phase

Glass transition temperature is influenced by the meta phenyl link content (Table I). The theoretical T_g of the 100% para PEKK, 165 °C, decreases about 9 °C, 6 °C, and 4 °C for PEKK 60/40, 70/30, and 80/20, respectively. The effect of meta linkages

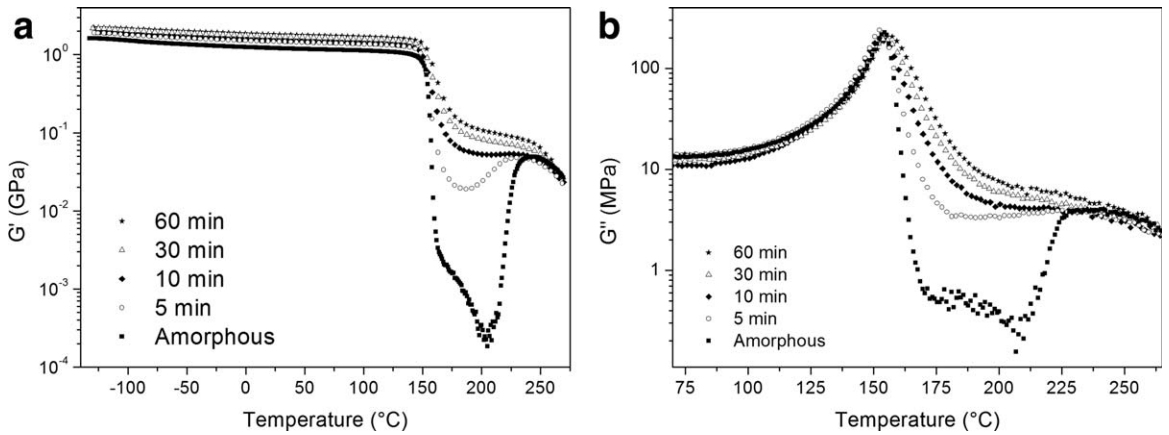

Figure 8. (a) G′ versus temperature at 1 rad s^{-1} for isothermally crystallized PEKK 60/40 at 245 °C during 5, 10, 30, and 60 min. (b) G″ vs temperature at 1 rad s^{-1} for isothermally crystallized PEKK 60/40 at 245 °C during 5, 10, 30, and 60 min.

Table III. T_∞ Crystallinity Ratio, and G′ Modulus Values of PEKK 60/40 after Annealing Process

Annealing time	T_α (°C)	G′ −125 °C (GPa)	G′ 0 °C (GPa)	G′ 125 °C (GPa)	G′ 150 °C (GPa)	χ (%)
5 min	153.5	1.9	1.5	1.3	0.9	10
10 min	153.5	2.0	1.6	1.4	0.9	20
30 min	155.0	2.2	1.8	1.5	1.2	25
60 min	157.5	2.2	1.9	1.6	1.4	27.5

has been already reported in the literature.[17,29] The decrease of T_g with the meta links was explained by the increase of the polymer chain flexibility. Only rapidly cooled samples for PEKK 80/20, 70/30 exhibit an endothermic peak superimposed on the glass transition. For PEKK 60/40 all samples exhibit this endothermic peak [Figure 3(a)]. For a given crystallinity ratio, polymer physical ageing[27,28] is classically observed for slow cooling rates. In this work, the magnitude of physical ageing decreases when cooling rates are lowered. The decrease can be explained by the high crystallinity ratios of the slow cooled samples: the local rearrangements of amorphous regions associated with physical ageing are restricted by crystallites.

Physical Structure: Crystalline Phase

The evolutions observed on crystallinity and melting temperature are directly linked to the variation of the T/I ratio (Table I). The 100% T PEKK has a high melting point between 385 °C and 400 °C,[17,30] close to the degradation temperature (about 400 °C). The melting point of the 100% meta linkages PEKK is close to 285 °C.[30] Increasing content of isophthalates moieties leads to a melting point decrease (Figure 2). The crystalline fraction of PEKK also decreases upon increasing of the meta content. Gardner *et al.*[17] and Hsiao *et al.*[29] evidenced that the incorporation of isophthalates moieties introduces asymmetry or entropy defects in the unit cell, generating such evolutions. The influence of meta linkages was also reported in others thermoplastic polymers with semi rigid chains e.g., works on polyesters reported by Hill *et al.*[31] They observed a reduction of melting point and crystallization ability in ethylene glycol polyesters derived from isophthalic acid compared with those derived from terephthalic acid. Moreover, Conix *et al.*[32] observed the same behavior in ethylene glycol polyesters: they attributed the reduction of crystallization ability to hindered rotation of meta phenyl groups by neighboring molecules, compared to para phenyl ones. In para linked poly(aryl ether ketones), the chain conformation in the crystal is a planar zigzag where the rings are torsionally rotated in opposite directions on either side of the ketone linkages. With the meta isomers introduction, some authors argue that the torsional rotation of phenyl rings disappeared within the crystal; contrary to para rings, the meta rings are aligned within the planar zigzag. This conformation, governed by the meta phenyl involves an energy penalty and thus, the reduction of melting temperature and crystallization rate.[33–35] As an example, Blundell[34] observed a reduction of 80 °C on melting temperature between a PEEKK and the PEEKmK (PEEK containing meta phenyl links).

Influence of Cooling Rates on the Physical Structure

Upon increasing cooling rates [Figure 3(a–c)], there is no evolution of melting temperature while the crystallinity content decreases: high cooling rates hinder the chain arrangement during the cooling from the melt. This evolution is observed in all the studied grades of PEKK, but the melt crystallized fraction of PEKK 60/40, is more susceptible to the cooling rate (Table I): the crystallization of PEKK 80/20 and 70/30 is faster than crystallization of PEKK 60/40. However, the crystallization rate from the melt is reduced by the introduction of meta linkages: the crystallinity fraction achieved by PEKK 60/40 at the slowest cooling rate is consequently lower than the one achieved for PEKK 80/20 and 70/30. By heating the highly amorphous samples, the beginning of cold crystallization is lower in temperature for PEKK 80/20 (190 °C) than for the 70/30 (200 °C) and the 60/40 (230 °C), proving that meta isomers increase the energy required to crystallize and hinder also the cold crystallization process.

A classical behavior is noticed on Table I: the enthalpy of cold crystallization increases when the polymer is subjected to fast cooling due to a higher percentage of crystallizable sequences in the amorphous phase. However, the quenched samples exhibit a singular behavior: the cold crystallization enthalpy is smaller than for others fast cooling rates. This decrease can be explained by a too low crystallization kinetic of crystallizable sequences due to the presence of isophthalate moieties.

Influence of Annealing on the Physical Structure

Annealing PEKK above T_g induces crystallization (Figures 4 and 5) as well as in other thermoplastic polymers.[21,23,36,37] A low temperature endotherm (LTE) appears on heating ramps at almost 10 °C above the annealing temperature. The high temperature endotherm (HTE) is not dependent from annealing protocols suggesting that the primary crystalline phase is not influenced by the evolutions occurring during the annealing. The double melting behavior in PEKK was already reported.[9,17] The LTE was already ascribed in PEKK to the melting of a secondary structure within the spherulite, evidenced by optical and small angle light scattering methods.[17] This behavior has also been observed several times in PEEK. Some hypotheses has been advanced to explain multiple endotherms. Crystal reorganization during heating was suggested as the origin of the LTE.[21,22,38] It was also reported that the origin of the low endotherm can be ascribed to the melting of less thermal stable crystallites in PEEK.[39,40] A strong dependence of the LTE with time and temperature is observed (Figures 4 and 5). Whatever annealing temperature, the difference between the annealing temperature and the LTE is about 10 °C. With increasing annealing time at a given temperature, the LTE temperature

increases. This increase can be associated with the crystal improvement due to conformational reorganizations during annealing.

Molecular Mobility in the Vitreous State

The main interest of PEKK is the nice vitreous plateau observed on the G′ dynamic mechanical thermogram before T_α. The vitreous plateau of G′ is slightly higher for PEKK 80/20 [Figure 6(a)]. The higher crystallinity associated to the higher value of T/I as shown on Figure 2, explain this evolution. In Figure 7, G′ during the second scan is slightly higher than the one measured during the first scan because of the achieved crystallinity during the heating process. Also in Figure 8(a), the increase of G′ modulus increases as well as isothermal crystallization time (annealing protocols). In these cases, a reinforcing effect on G′ at the glassy state by crystallites is observed. Crystallites rigidify the material, but the reinforcing effect of the vitreous plateau is low. This reinforcing effect before T_α was also reported in PET.[41,42] Here, crystallites could act as fillers in a based polymer composite material, where an increase of G′ modulus in the glassy state is a frequently classical behavior observed.[13,43]

Concerning the G″ [Figure 6(b)], no evolution with the T/I ratio is observed: the maxima temperatures and the amplitudes of the sub-T_α relaxation peaks are unchanged. Moreover, we mentioned that the crystallinity does not influence the sub-T_α relaxations [Figure 7(b)]. This is an expected behavior considering that the sub-T_α relaxations are located in the amorphous phase. The γ and β relaxation of PEKK has only been reported by dielectric techniques.[26,44] Generally, a broad β transition was observed in the same range of temperature that our γ mechanical relaxation. Sauer *et al.* reported in PEKK two sub glass relaxations: γ at −135 °C and β at −70 °C for amorphous and semicrystalline samples at 1 KHz. A reduction of 25% of magnitude for the β relaxation was observed in a crystalline PEKK compared with an amorphous one.[44] They suggested that the β relaxation is due to local segmental motions in the amorphous phase but any molecular origin was assigned. Moreover, Goodwin *et al.*[26] reported a relaxation in PEKK at −50 °C and its sensitivity to absorbed moisture: the temperature and amplitude increase with the absorbed water content.[26] Furthermore, sub-T_α relaxations have been extensively studied in PEEK and PEK by dynamical mechanical analysis.[26,45–47] A broad relaxation mode was observed in the same temperature range that our γ mode. Sasuga *et al.* reported a broad γ mode in PEEK at −75 °C associated to the local motion of phenylene units in the main chain.[46] David *et al.* reported a bimodal β relaxation resulting of two components: β_1 at −110 °C corresponding to phenyl mobility around their axes and β_2 at −33 °C ascribed to interchain cooperative mobility.[47] Bas *et al.*[48] suggested that the β_1 component at about −80 °C results from mobility of polar entities that can complex with absorbed water. Finally, Goodwin suggested that in PAEKs there is little influence of chemical structure on the shape, location, and relaxation behavior of the β mode.[26] Since the chemical structure of PEKK and PEEK are closed, the γ and β relaxations could be assigned to the mobility of polar entities and phenylene units in the main chain, respectively.

Viscoelastic Relaxation

G′ of all PEKK grades is more affected by crystalline fraction in the T_α region. After 150 °C the sudden drop of G′ associated to the viscoelasticity is more pronounced for PEKK 60/40 and 70/30 than for 80/20 due to high differences in crystalline fraction. Similar behavior has been reported for amorphous and semi crystalline PEEK from DMA analyses. The drop of the G′ at the viscoelastic transition of an amorphous PEEK was about two decades at 10 Hz[24] and 2.5 decades at 0.1 Hz.[25] After the drop, for PEKK 60/40 and 70/30 the rubbery plateau decreases until the beginning of the cold crystallization process. With such a low value of crystallinity, the sudden decrease of G′ results in a flow behavior. Without enough crystalline fraction achieved, between 150 °C and 190 °C for PEKK 70/30 and 150 °C and 210 °C for PEKK 60/40, the mechanical properties are very low: the limit of sensitivity of the apparatus is reached. For semicrystalline PEKK 80/20, the drop of only of 1 decade [Figure 6(a)] is consistent with results of semicrystalline PEEK at 10 Hz,[24] and between 0.2 and 1 Hz.[46] After the step, a "classical" rubbery plateau is observed.

For the G″, it was observed in DMA that the α mode broadens towards higher temperatures [Figure 8(b)] with increasing crystallinity. Previous observations were already reported where the α mode broadens in PEEK[24,45] and PET,[41] due to the long range segmental motions restrictions in the amorphous phase. In fact, whereas larger crystallites are created with increasing annealing time, the interface between amorphous regions and crystal regions increase, the polymers chains mobility around the interfaces decrease, increasing the percentage of constrained phase with low mobility. Therefore, this constrained phase exhibits an α relaxation at higher temperatures and is responsible for the asymmetrical broadening of mean α mode. This phase is associated to the rigid amorphous fraction (RAF) developed in cold crystallized semi-crystalline polymers as revealed by DSC analysis.[49,50] No evolution of the intensity and the maximum temperature is observed, proving that the rest of amorphous phase is not influenced by crystalline phase.

Molecular Mobility in the Rubbery State

The increase of the G′ on the rubbery plateau for PEKK 60/40 and 70/30 is directed linked with the cold crystallization. The temperature range corresponds to the cold crystallization transition observed in DSC Figure 3(a,b)]. This behavior was previously observed by DMA for PEEK[24,25] and for other amorphous polymers containing terephthalate moieties such as PET.[51] The rubbery plateau position is related to newly created crystallites.[52] Crystallites act as reinforcing fillers, due to ties between amorphous and crystalline phases. With increasing annealing times, the crystalline phase increases together with the reinforcing effect in G'. For long annealing times, the quasi-maximum crystallinity is reached and a horizontal rubbery plateau is observed. The G″ also increases during cold crystallization process [Figures 7(b) and 8(b)]. This increase reveals a rise in dissipated energy. Throughout the cold crystallization, new crystallites are created and the interface content between crystalline and amorphous material rises. Mechanical friction at this interface can be responsible of this energy loss.

CONCLUSIONS

The aim of this work was to define the influence of asymmetry of the PEKK chains on processing conditions and on the mechanical performances of the polymer. The influence of the T/I isomer ratio and thermal history of various grades of PEKK were studied by differential scanning calorimetry and dynamic mechanical analysis. In the glassy state, two γ and β relaxations were observed on the temperature variation of G″; they correspond to the mobility in the vitreous state of polar and phenylene units respectively. In the vitreous state, no particular effect of the T/I ratio was observed on G″: localized molecular mobility in the amorphous phase is not influenced by such configurations.

It was noticed that the temperature of the viscoelastic transition, T_α, slowly decreases for increasing meta link content. Similar results were reported for the glass transition measured by DSC. In other words, the cohesion of the amorphous phase is slightly weakened by meta isomer moieties.

It is interesting to note that the physical ageing phenomenon on PEKK strongly depends on crystallinity, more than thermal history: there is a strong coupling of amorphous and crystalline phases.

The T/I ratio has a strong influence on the melting temperature: the decrease of melting point was about 60 °C between PEKK 80/20 and 60/40. Consequently, the introduction of meta isomers improves processability. We also confirmed that isophthalate moieties prevent crystallinity: for the same thermal history, crystallinity of PEKK 70/30 and 60/40 are lower than for PEKK 80/20.

However, regardless the T/I ratio, PEKK can be obtained in the amorphous or semicrystalline state, depending on the processing conditions. The double melting behavior was observed after an annealing at a temperature beyond the glass transition that might favor new interchain interactions. The low temperature endotherm depends on annealing time and temperature. The effect of crystallinity on dynamic mechanical properties was also studied. No influence was observed on the relaxations modes with annealing time or crystallinity. In the vicinity of the glass transition, the crystallinity prevents the loss of cohesion. Even if a small effect is recorded on the glassy plateau, the effect of crystallinity is more prominent on the rubbery plateau. The T/I isomer ratio facilitates processing of PEKK while maintaining mechanical performances.

ACKNOWLEDGMENTS

The authors gratefully acknowledge the financial support of BPI/F and Conseil Régional Midi Pyrénées/F through the COSMIC program.

REFERENCES

1. Diez-Pascual, A. M.; Naffakh, M.; Marco, C.; Ellis, G.; Gomez-Fatou, M. A. *Progr. Mater. Sci.* **2012**, *57*, 1106.
2. Chang, I. Y. *Sampe Quart.* **1988**, *19*, 29.
3. Kemmish, D. Technology and Applications of Polyaryletherketones, iSmithers **2010**.
4. Pilato, L. A.; Michno, M. J. *Adv. Compos. Mater.* Springer-Verlag **1994**.
5. Seferis, J. C. *Polym. Compos.* **1986**, *7*, 158.
6. Lee, Y.; Porter, R. S. *Polym. Eng. Sci.* **1986**, *26*, 633.
7. Carponcin, D.; Dantras, E.; Laffont, L.; Dandurand, J.; Aridon, G.; Levallois, F.; Cadiergues, L.; Lacabanne, C. *J. Non-Cryst. Solids* **2014**, *388*, 32.
8. Goyal, R. K.; Negi, Y. S.; Tiwari, A. N. *Eur. Polym. J.* **2005**, *41*, 2034.
9. Chang, I. Y.; Hsiao, B. S. 36th International SAMPE symposium, 1587 **1991**.
10. Gan, D.; Lu, S.; Song, C.; Wang, Z. *Eur. Polym. J.* **2001**, *37*, 1359.
11. Hsiao, B. S.; Chang, I. Y.; Sauer, B. B. *Polymer* **1991**, *32*, 2799.
12. Gan, D. J.; Cao, W. J.; Song, C. S.; Wang, Z. J. *Mater. Lett.* **2001**, *51*, 120.
13. Gan, D. J.; Lu, S. Q.; Song, C. S.; Wang, Z. J. *Mater. Lett.* **2001**, *48*, 299.
14. Brugel, E. G. EP0225144 A2 **1986**.
15. Jog, J. P.; Nadkarni, V. M. *J. Appl. Polym. Sci.* **1986**, *32*, 3317.
16. Abraham, R. J.; Haworth, I. S. *Polymer* **1991**, *32*, 121.
17. Gardner, K. H.; Hsiao, B. S.; Matheson, R. R.; Wood, B. A. *Polymer* **1992**, *33*, 2483.
18. Bai, J. M.; Leach, D.; Pratte, J. *JEC Composites* **2005**, *15*, 64.
19. Medellinrodriguez, F. J.; Phillips, P. J. *Polym. Eng. Sci.* **1990**, *30*, 860.
20. Lee, Y. C.; Porter, R. S. *Macromolecules* **1988**, *21*, 2770.
21. Blundell, D. J.; Osborn, B. N. *Polymer* **1983**, *24*, 953.
22. Lee, Y. C.; Porter, R. S. *Macromolecules* **1987**, *20*, 1336.
23. Roberts, R. C. *Polymer* **1969**, *10*, 117.
24. Damore, A.; Kenny, J. M.; Nicolais, L.; Tucci, V. *Polym. Eng. Sci.* **1990**, *30*, 314.
25. Krishnaswamy, R. K.; Kalika, D. S. *Polymer* **1994**, *35*, 1157.
26. Goodwin, A. A.; Hay, J. N. *J. Polym. Sci. B: Polym. Phys.* **1998**, *36*, 851.
27. Struik, L. C. E. *Polym. Eng. Sci.* **1978**, *17*, 165.
28. Hutchinson, J. M. *Progr. Polym. Sci.* **1995**, *20*, 703.
29. Hsiao, B. S.; Gardner, K. H.; Cheng, S. Z. D. *J. Polym. Sci. B Polym. Phys.* **1994**, *32*, 2585.
30. Ke, Y.; Wu, Z. *J. Appl. Polym. Sci.* **1998**, *67*, 659.
31. Hill, R.; Walker, E. E. *J. Polym. Sci.* **1948**, *3*, 609.
32. Conix, A.; Van Kerpel, R. *J. Polym. Sci.* **1959**, *40*, 521.
33. Blundell, D. J.; Liggat, J. J.; Flory, A. *Polymer* **1992**, *33*, 2475.
34. Blundell, D. J. *Polymer* **1992**, *33*, 3773.
35. Ho, R. M.; Cheng, S. Z. D.; Hsiao, B. S.; Gardner, K. H. *Macromolecules* **1995**, *28*, 1938.
36. Bell, J. P.; Slade, P. E.; Dumbleton, J. H. *J. Polym. Sci. 2 Polym. Phys.* **1968**, *6*, 1773.
37. Samuels, R. J. *J. Polym. Sci. B: Polym. Phys.* **1975**, *13*, 1417.

38. Blundell, D. J. *Polymer* **1987**, *28*, 2248.
39. Bassett, D. C.; Olley, R. H.; Alraheil, I. A. M. *Polymer* **1988**, *29*, 1745.
40. Cheng, S. Z. D.; Cao, M. Y.; Wunderlich, B. *Macromolecules* **1986**, *19*, 1868.
41. Illers, K. H.; Breuer, H. *J. Colloid Sci.* **1963**, *18*, 1.
42. Shieh, Y. T.; Lin, Y. S.; Twu, Y. K.; Tsai, H. B.; Lin, R. H. *J. Appl. Polym. Sci.* **2010**, *116*, 1334.
43. Quiroga Cortes, L.; Lonjon, A.; Dantras, E.; Lacabanne, C. *J. Non-Cryst. Solids* **2014**, *391*, 106.
44. Sauer, B. B.; Avakian, P.; Starkweather, H. W.; Hsiao, B. S. *Macromolecules* **1990**, *23*, 5119.
45. Jonas, A.; Legras, R. *Macromolecules* **1993**, *26*, 813.
46. Sasuga, T.; Hagiwara, M. *Polymer* **1986**, *27*, 821.
47. David, L.; Etienne, S. *Macromolecules* **1992**, *25*, 4302.
48. Bas, C.; Alberola, N. D. *Polym. Eng. Sci.* **1996**, *36*, 244.
49. Henricks, J.; Boyum, M.; Zheng, W. *J. Therm. Anal. Calorim.* **2015**, *120*, 1765.
50. Xu, H.; Ince, B. S.; Cebe, P. *J. Polym. Sci. B: Polym. Phys.* **2003**, *41*, 3026.
51. Dong, W.; Zhao, J.; Li, C. X.; Gu, M. L.; Zhao, D. L.; Fan, Q. R. *Polym. Bull.* **2002**, *49*, 197.
52. Menard, K. P. An Introduction to Dynamic Mechanical Analysis, CRC Press LLC **1999**.